ELSEVIER

www.elsevier.nl/locate/jorganchem

Journal of Organometallic Chemistry 612 (2000) 61–68

Journal of Organometallic Chemistry

The photolysis of $Fe(CO)_3\{P(OPh)_3\}_2$ and reaction of the photoproduct with alkynes: crystal structures of $Fe(CO)_2\{P(OPh)_3\}_2(\eta^2\text{-PhCCPh})$, $Fe(CO)_2\{P(OPh)_3\}_2\{\eta^1{:}\eta^1\text{-C(O)C(Me)C[CH(OEt)}_2\text{]C(O)}\}$ and $Fe_2(CO)_4\{P(OPh)_3\}_2(PhCCH)_2$

M. Barrow [a], N.L. Cromhout [a], D. Cunningham [b], A.R. Manning [a,*], P. McArdle [b]

[a] *Department of Chemistry, University College Dublin, Belfield, Dublin 4, Ireland*
[b] *Department of Chemistry, University College Galway, Galway, Ireland*

Received 11 May 2000; received in revised form 15 June 2000

Abstract

UV-irradiation of $Fe(CO)_3\{P(OPh)_3\}_2$ (**1**) afforded an orthometallated iron hydride $HFe(CO)_2\{P(OPh)_3\}\{(PhO)_2POC_6H_4\}$ (**2**) which was reacted in situ with alkynes $R^1C{\equiv}CR^2$. Internal alkynes reacted to give either η^2-alkyne $Fe(CO)_2\{P(OPh)_3\}_2(\eta^2\text{-}R^1CCR^2)$ [**3a**, $R^1 = R^2 = Ph$; **3b**, $R^1 = Ph$, $R^2 = CH(OEt)_2$] or maleoyl $Fe(CO)_2\{P(OPh)_3\}_2\{\eta^1{:}\eta^1\text{-C(O)C}(R^1)\text{C}(R^2)\text{C(O)}\}$ [**4a**, $R^1 = Ph$, $R^2 = Me$; **4b**, $R^1 = R^2 = Me$; **4c**, $R^1 = Me$, $R^2 = CH(OEt)_2$; **4d**, $R^1 = Me$, $R^2 = CH_2OH$; **4e**, $R^1 = R^2 = CH_2OH$] complexes. The terminal alkyne HC≡CPh reacted with **2** to give the ferrole derivative $Fe_2(CO)_4\{P(OPh)_3\}_2(PhCCH)_2$ (**5**). The crystal structures of **3a**, **4c** and **5** were determined. Complex **3a** is trigonal bipyramidal about the iron atom with trans apical phosphite ligands and an equatorial arrangement of the CO groups and alkyne CC moiety. Complex **4c** is octahedral with trans phosphite ligands and cis carbonyl groups. The alkyne ligand has undergone double carbonylation to generate a ferracyclopentenedione (maleoyl) ring that occupies the remaining two coordination sites at the metal centre. Complex **5** is formally a derivative of $Fe_2(CO)_9$ in which an $Fe(CO)_2\{P(OPh)_3\}$ moiety is π-bonded to a ferracyclopentadiene ring arising from the tail-to-tail coupling of two HC≡CPh ligands.

Keywords: Iron carbonyl; Phosphite; Orthometallation; Alkyne; Maleoyl; Ferrole

1. Introduction

The reactions of iron carbonyls with alkynes afford a wealth of organometallic derivatives with a diverse array of structures [1] and with numerous practical applications to organic synthesis [2]. All too often, however, these reactions are plagued by a lack of selectivity. Complex mixtures leading to a myriad of reaction products are obtained and reaction mechanisms are often unclear. In this paper we describe the photolysis of the iron carbonyl $Fe(CO)_3\{P(OPh)_3\}_2$ and show that the reactions of alkynes with the photoproduct $HFe(CO)_2\{P(OPh)_3\}\{(PhO)_2POC_6H_4\}$ proceed selectively to afford only one of three product types depending on the acetylenic substituents.

2. Results and discussion

The chemistry of $Fe(CO)_3\{P(OPh)_3\}_2$ (**1**) is relatively under-represented in the literature compared to that of its phosphine analogue $Fe(CO)_3(PPh_3)_2$ for which convenient and high yielding syntheses are available [3]. Literature methods for the preparation of **1** give this complex in only ca. 15% yield [4]. We now report that reflux of $Fe(CO)_5$ with $P(OPh)_3$ in mesitylene followed by addition of methanol to the cooled reaction mixture, afforded **1** in ca. 65% yield with no contamination from

* Corresponding author. Tel.: +353-1-7062311; fax: +353-1-7062127.
E-mail address: anthony.manning@ucd.ie (A.R. Manning).

0022-328X/00/$ - see front matter
PII: S0022-328X(00)00384-3

$Fe(CO)_4\{P(OPh)_3\}$. The crystal structure of **1** has recently been described [5].

Previous work from this laboratory has shown that the photolysis of **1** results in CO loss and the formation of a new compound **2**, which may be isolated as a moderately air-sensitive oil [6]. The structure of **2** was deduced from its IR spectrum (two high frequency ν_{CO} bands at 2034 and 1986 cm^{-1} indicating *cis* carbonyl ligands and an oxidised metal centre) and from its subsequent reactions with a variety of ligands (see below). It was formulated as the orthometallated iron hydride $HFe(CO)_2\{P(OPh)_3\}\{(PhO)_2POC_6H_4\}$; this assignment is supported by ^{1}H-NMR spectroscopic data: a broadened multiplet centred at δ −9.36 is attributable to the metal-bound H ligand.

In the presence of two-electron donor ligands L, complex **2** undergoes an intramolecular reductive elimination (deorthometallation) and ligand addition to afford Fe^0 complexes $Fe(CO)_2\{P(OPh)_3\}_2(L)$. With substrates such as HCl or H_2, Fe^{II} complexes $Fe(CO)_2\{P(OPh)_3\}_2(X)(Y)$ (X = H; Y = H, Cl) are obtained [6]. This latter mode of reactivity was exploited by Schubert and co-workers to prepare derivatives with X = H and Y = SiR_3 [7].

We describe here the reactions of $HFe(CO)_2\{P(OPh)_3\}\{(PhO)_2POC_6H_4\}$ (**2**) with a series of alkyne ligands; these reactions are summarised in Scheme 1. In a typical procedure, a stoichiometric amount of the alkyne was added to a toluene solution of **2**, generated in situ by UV-irradiation of **1**, and the mixture was allowed to stir at room temperature overnight. A single product was obtained in each instance although isolated yields were generally modest. It was found, however, that the yields of **3** and **4** were improved if the reactions were conducted in the presence of a Lewis acid: for example, an increase in yield from 12 to 65% of the isolated product **3a** was obtained on addition of hydrated $ZnCl_2$ to the reaction of **2** with diphenylacetylene. Anhydrous $ZnCl_2$ compromised both the yield and selectivity of the reaction affording ca. 25% **3a** and other unidentified products. For the acetal-functionalised alkynes, addition of $ZnCl_2{\cdot}nH_2O$ afforded the alkyne–aldehyde and $Fe(CO)_2(Cl)_2\{P(OPh)_3\}_2$, identified by comparison with an authentic sample. For these reactions anhydrous $MgSO_4$ was therefore employed as Lewis acid. The mode of action of these additives is not clear to us presently. The yields, melting points, analyses and infra-

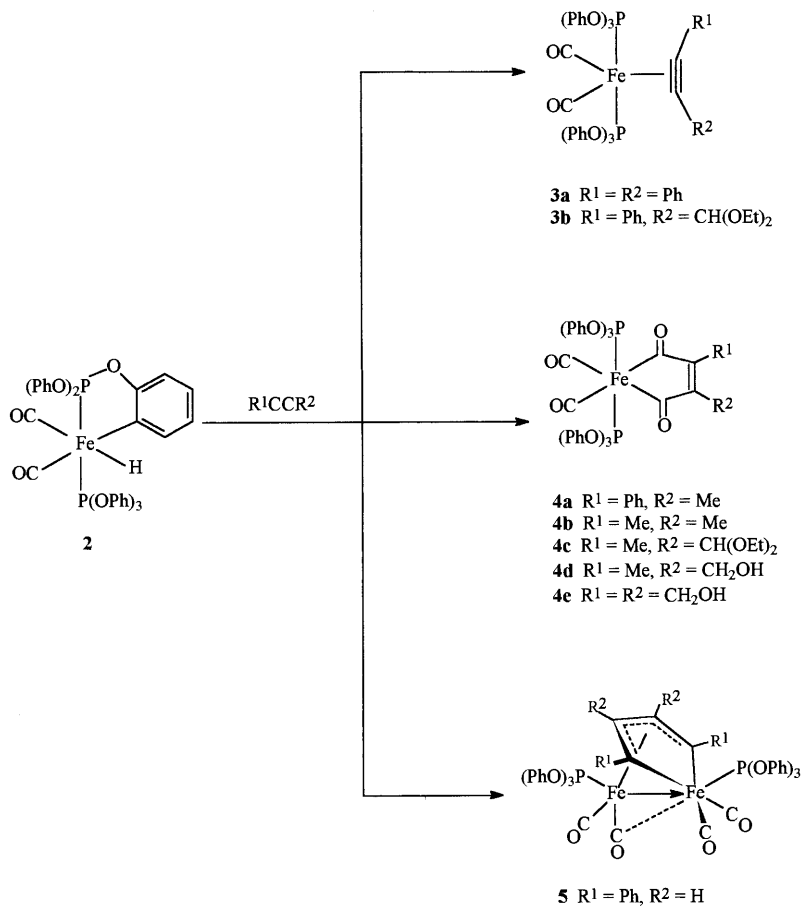

Scheme 1. Reactions of $HFe(CO)_2\{P(OPh)_3\}\{(PhO)_2POC_6H_4\}$ (**2**) with alkynes R^1CCR^2.

Table 1
Yields, melting points, analyses and infrared spectral data for **3–5**

Compound	Yield	M.p.	Analyses [a]			IR spectra [b]	
	(%)	(°C)	%C	%H	%P	ν(C≡O)	Other
3a	65	125–126	68.2(68.6)	4.5(4.4)	7.1(6.8)	1980(8.0), 1914(10)	ν(C≡C) 1827(3.1)
3b	56	85	64.1(64.9)	4.1(5.0)	6.9(6.7)	2000(5.8), 1934(10)	ν(C≡C) 1789(1.2)
4a	43	144–146	65.1(65.1)	4.4(4.2)	7.0(6.9)	2041(9.4), 1987(10)	ν(C=C) 1606(3.1), ν(C=O) 1618(4.6)
4b·$\frac{1}{2}CH_2Cl_2$ [c]	48	135–136	59.6(60.4)	4.3(4.2)	7.6(7.0)	2045(9.2), 1994(10)	ν(C=C) 1605(3.1), ν(C=O) 1618(4.2)
4c	39	121–122	62.9(62.0)	4.5(4.8)	7.7(6.7)	2039(7.4), 1983(10)	ν(C=C) 1606(2.8), ν(C=O) 1621(2.4)
4d	38	120–121	61.6(61.6)	4.1(4.2)	7.0(7.2)	2040(8.3), 1985(10)	ν(C=C) 1606(3.6), ν(C=O) 1621(2.8)
4e	42	144–146	59.9(60.4)	4.1(4.2)	7.1(7.1)	2040(9.1), 1985(10)	ν(C=O) and ν(C=O) 1610(6.7)
5·$\frac{1}{2}CH_2Cl_2$ [c]	42	101–102	62.8(62.2)	3.8(4.0)	5.7(5.7)	2009(7.5), 1978(10) 1930(6.2), 1920(sh) [d]	

[a] Found with calculated values in parentheses.
[b] Spectra recorded as KBr disks; values in cm^{-1} with relative peak heights in parentheses.
[c] Contains $\frac{1}{2}CH_2Cl_2$ of crystallisation.
[d] sh = shoulder.

Table 2
NMR spectroscopic data for **3–5**

Compound	Nucleus	Spectral data [a]
3a	^{1}H [b]	7.50–6.85 (m, Ph)
	^{13}C [c]	217.8 (br [d] s, CO), 151.6–121.1 (Ph), 91.9 (br s, C≡C)
	^{31}P [e]	152.6 (s)
3b	^{1}H	7.49–6.86 (m, 35H, Ph), 5.50 (s, 1H, CH), 3.83 (m, 2H, 2× C*H*HCH$_3$), 3.70 (m, 2H, 2× CH*H*CH$_3$), 1.28 (t, 6H, CH$_3$)
	^{13}C	215.8 (br s, CO), 215.1 (br s, CO), 151.0–120.6 (Ph), 85.7 (br s, *C*≡C), 84.9 (br s, C≡*C*), 92.3 (s, CH), 61.4 (s, CH$_2$), 15.7 (s, CH$_3$)
4a	^{1}H	7.21–6.90 (m, 35H, Ph), 1.79 (s, 3H, CH$_3$)
	^{13}C	261.1 (t, $^2J_{CP}$ = 31 Hz, C=O), 258.7 (t, $^2J_{CP}$ = 30 Hz, C=O), 206.2 (m, 2×C≡O), 167.4 (s, *C*=C), 167.1 (s, C=*C*), 151.0–121.1 (Ph), 12.8 (s, CH$_3$)
4b	^{1}H	7.42–6.78 (m, 30H, Ph), 1.65 (s, 6H, CH$_3$)
	^{13}C	260.5 (t, $^2J_{CP}$ = 30 Hz, C=O), 206.0 (t, $^2J_{CP}$ = 20 Hz, C≡O), 162.1 (s, *C*=*C*), 151.0–120.8 (Ph), 13.58 (s, CH$_3$)
4c	^{1}H	7.35–6.70 (m, 30H, Ph), 5.59 (s, 1H, CH), 3.57 (m, 2H, 2× C*H*HCH$_3$), 3.36 (m, 2H, 2× CH*H*CH$_3$), 2.05 (s, 3H, C=CCH$_3$), 1.00 (t, 6H, J_{HH} = 7.1 Hz, CH$_2$C*H*$_3$)
	^{13}C	261.3 (t, $^2J_{CP}$ = 30 Hz, C=O), 259.7 (t, $^2J_{CP}$ = 30 Hz, C=O), 206.4 (t, $^2J_{CP}$ = 24 Hz, C≡O), 206.1 (t, $^2J_{CP}$ = 24 Hz, C≡O), 169.9 (s, *C*=C), 162.8 (s, C=*C*), 151.5–121.4 (Ph), 98.0 (s, CH), 63.3 (s, CH$_2$), 15.4 (s, CH$_2$*C*H$_3$), 12.0 (s, CH$_3$)
	^{31}P	145.2 (s)
4d	^{1}H	7.36–6.90 (m, 30H, Ph), 4.36 (s, 2H, CH$_2$), 3.43 (s, 1H, OH), 1.65 (s, 3H, CH$_3$)
	^{13}C	259.1 (t, $^2J_{CP}$ = 31 Hz, C=O), 258.0 (t, $^2J_{CP}$ = 31 Hz, C=O), 206.0 (t, $^2J_{CP}$ = 20 Hz, C≡O), 205.2 (t, $^2J_{CP}$ = 20 Hz, C≡O), 165.0 (s, *C*=C), 161.8 (s, C=*C*), 151.0–120.1 (Ph), 59.1 (s, CH$_2$), 11.1 (s, CH$_3$)
4e	^{1}H	7.26–6.91 (m, 30H, Ph), 4.36 (s, 4H, CH$_2$), 3.08 (s, 2H, OH)
	^{13}C	261.3 (t, $^2J_{CP}$ = 29 Hz, C=O), 205.7 (t, $^2J_{CP}$ = 21 Hz, C≡O), 165.4 (s, *C*=*C*), 151.2–120.7 (Ph), 58.0 (s, CH$_2$)
5	^{1}H	7.39–6.38 (m, Ph)
	^{13}C	217.9 (br d, $^2J_{CP}$ = 27.3 Hz, Fe2–CO), 209.0 (br d, $^2J_{CP}$ = 23.7 Hz, Fe1–CO) 172.2 (br d, $^2J_{CP}$ = 15.1 Hz, 2× CPh), 151.3–120.8 (Ph), 107.6 (s, 2×CH)
	^{31}P	170.3 (s), 161.9 (s)

[a] Obtained in $CDCl_3$ solution; chemical shifts in ppm.
[b] 270 MHz; referenced to tetramethylsilane.
[c] 67.8 MHz; referenced to internal $CDCl_3$.
[d] br = broad.
[e] 121 MHz; referenced to 85% phosphoric acid in D_2O with downfield shifts reported as positive.

red spectral data of the products are presented in Table 1; NMR spectroscopic data are contained in Table 2.

2.1. η^2-Alkyne complexes

The simple ligand-addition products $Fe(CO)_2\{P(OPh)_3\}_2(L)$ **3** were obtained only for L = PhC≡CPh and $PhC{\equiv}CCH(OEt)_2$. The structures of **3** were inferred from the infrared and NMR spectroscopic data: in particular, a band at 1827 cm^{-1} in the IR spectrum of **3a** was identified as a $\nu_{C\equiv C}$ stretching frequency by comparison with that reported for $Fe(CO)_2\{P(OMe)_3\}_2$(PhCCPh) (**6**) ($\nu_{C\equiv C}$ = 1832 cm^{-1}) [8]. The ^{13}C-NMR spectrum of **3a** exhibits broadened resonances for both the carbonyl and acetylenic carbon atoms at δ 217.8 and 91.9, respectively; that of **3b**, which contains the unsymmetrical alkyne $PhC{\equiv}CCH(OEt)_2$, exhibits separate but broadened carbonyl carbon resonances (δ 215.8 and 215.1) suggesting the possibility of a dynamic process in this complex at temperatures above ambient.

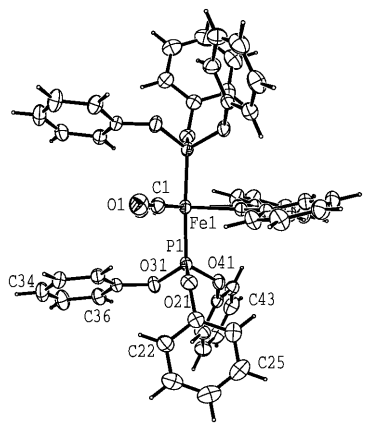

Fig. 1. ORTEX diagram of the molecular structure of **3a**. Selected bond lengths (Å) and angles (°): Fe–P1, 2.1702(5); Fe–C1, 1.769(2); Fe–C2, 2.0566(16); C2–C2′, 1.274(4); C2–C11, 1.447(3); P1–Fe–$P1_1$, 177.04(2); C1–Fe1–$C1_1$, 111.06(12); C1–Fe–C2, 142.35(8); C2–Fe–$C2_1$, 36.10(11); Fe–P1–O21, 112.20(5); Fe–P1–O31, 120.58(6); Fe–P1–O41, 118.20(5). Symmetry operator ′ = $-x$, y, $1/2-z$.

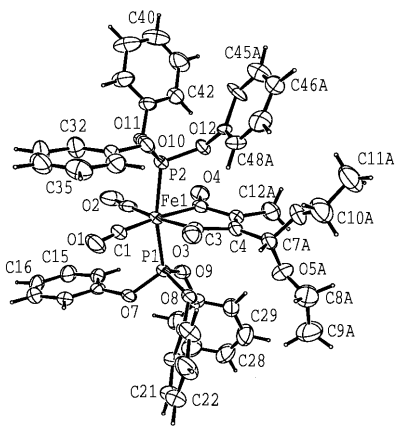

Fig. 2. ORTEX diagram of the molecular structure of **4c** (major conformation). Selected bond lengths (Å) and angles (°): Fe–P1, 2.1631(12); Fe–P2, 2.1747(12); Fe–C1, 1.812(4); Fe–C2, 1.773(8); Fe–C3, 1.959(7); Fe–C6, 2.004(5); C3–C4, 1.520(6); C4–C5, 1.321(7); C5–C6, 1.503(7); C3–O3, 1.247(6); C6–O4, 1.222(6); P1–Fe–P2, 167.89(4); C1–Fe–C2, 97.4(2); C2–Fe–C6, 91.6(3); C3–Fe–C6, 80.8(2); C1–Fe–C3, 90.3(2); Fe–C6–C5, 113.8(4); Fe–C3–C4, 115.4(5).

The structure of **3a** was determined by an X-ray diffraction study. The molecule resides on a crystallographic two-fold axis containing the iron atom and bisecting the alkyne ligand. An ORTEX [9] diagram of the molecule is shown in Fig. 1 with selected bond lengths and angles. The configuration about the central iron atom is approximately trigonal bipyramidal with the phosphite ligands occupying the trans apical sites [P–Fe–P bond angle = 177.04(2)°]. The Fe–P bond distances at 2.1702(5) Å are substantially lengthened compared to the parent tricarbonyl complex **1** which has Fe–P = 2.1408(8) and 2.1421(8) Å [5]. The asymmetry of the phosphite ligands noted in **1** is also observed in **3a** where one of the Fe–P–O bond angles at 112.20(5)° is considerably smaller than the remaining two [118.20(5) and 120.58(6)°].

The carbonyl ligands and the acetylenic CC moiety comprise the equatorial plane of the molecule. The distance from the Fe atom to the centroid of the η^2-diphenylacetylene is 1.9554(15) Å and the bite angle (C2–Fe–C2′) of this ligand is 36.10(11)°. The alkyne is bent into *cis* geometry with a Ph–C–C angle of 148.42(9)°, which may be compared with a value of 148.9(2)° in **6**. These Ph–C–C angles are at the upper end of a range of 135–154° reported for the diphenylacetylene ligand in mononuclear metal complexes [10]; the larger the angle, the smaller the deviation from the ideal linear geometry of the free PhC≡CPh ligand. The CC bond length in **3a** is 1.274(4) Å and is comparable to that in **6** [1.263(6) Å]; these values lie towards the shorter end of the reported range of coordinated diphenylacetylene CC distances of 1.24–1.35 Å [10].

2.2. Maleoyl complexes

Complexes **4a**–**e** were obtained on reaction of **2** with the internal alkynes listed in Scheme 1. These species are distinguished by considerably higher ν_{CO} stretching frequencies (Table 1) than for the η^2-alkyne complexes **3** and by the absence of any IR bands attributable to an acetylenic CC group. Instead, weak IR absorption bands at ca. 1606 cm^{-1} and ^{13}C-NMR signals in the region 160–165 ppm indicated the presence of olefinic carbons and suggested that oligomerisation of the alkyne had occured. In fact, these compounds were identified as ferracyclopentenedione complexes by an X-ray diffraction analysis of a representative example, **4c**.

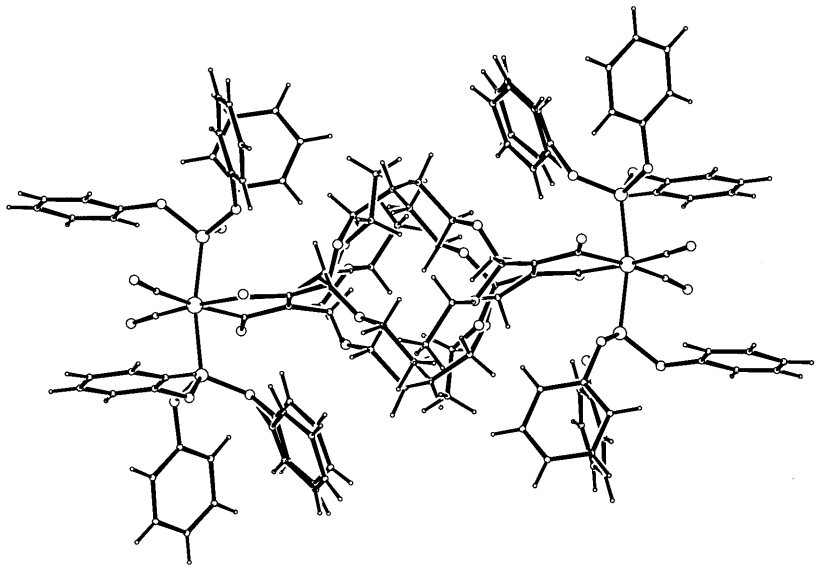

Fig. 3. A view of two symmetry-related molecules of **4c** depicting the maleoyl disorder.

An ORTEX diagram of the major conformation (the disorder is described below) of molecule **4c** is shown in Fig. 2 together with selected bond lengths and angles. The alkyne ligand has undergone double carbonylation to generate a five-membered maleoyl-type metallacycle. The bonding within this ring is similar to that in the related compounds $Fe(CO)_4[\eta^1{:}\eta^1\text{-}C(O)C_2Et_2C(O)]$ (**7**) [11] and $Fe(CO)_4[\eta^1{:}\eta^1\text{-}C(O)C(Me)C(C_2Me)C(O)]$ (**8**) [12]. There is no evidence for delocalisation in the ring: C4–C5 [1.321(7) Å] is a typical C–C double bond; C3–C4 [1.520(6) Å] and C5–C6 [1.503(7) Å] are single bonds. The Fe–CO (ketonic) bond lengths of 1.959(7) and 2.004(5) Å are in the range of values found for Fe^{II}–C(sp^2) bonds, although slightly shorter than the mean value (2.05 Å) [13] and the corresponding distances in both **7** (mean 2.009 Å) and **8** (mean 2.024 Å). The relative electron richness of the $Fe(CO)_2\{P(OPh)_3\}_2$ fragment compared to $Fe(CO)_4$ may account for the more strongly deshielded ^{13}C-NMR resonance of these carbons (ca. δ 260) compared to those in **7** and **8** (ca. δ 240). The distances C3–O3 [1.247(6) Å] and C6–O4 [1.222(6) Å] are slightly, but not significantly, longer than normal C=O bonds (1.21 Å) [13]. The coordination about the Fe^{II} centre is completed by two CO ligands co-planar with the maleoyl ring and by two trans phosphites above and below this plane. Distortions from octahedral geometry are relatively small apart from the C3–Fe–C6 angle of 80.8(2)° imposed by the ring [and the correspondingly large C1–Fe–C2 angle of 97.4(2)°] and a significant displacement of the *trans* phosphite ligands in the direction of the ring [P1–Fe–P2 = 167.89(4)°]. This inclination of the axial ligands appears to be a common feature of iron-maleoyl structures [11,12,14].

The maleoyl residue in molecule **4c** adopts two distinct orientations in the asymmetric unit of the crystal structure. In the average structure, the conformation $(EtO)_2CH$–C(4)=C(5)–Me represents the major maleoyl orientation (0.805 site occupancy) and is superimposed upon Me–C(4)=C(5)–$CH(OEt)_2$, the minor orientation (remaining 0.195 site occupancy). Molecules of **4c** crystallise such that the maleoyl groups of neighbouring molecules reside about an inversion centre and in close proximity; a dimer showing the disorder is depicted in Fig. 3. Phenyl rings surround this disorder volume element.

2.3. Ferrole complexes

The binuclear iron ferrole **5** is the third structural type observed in this study. Ferrole complexes are amongst the most common of the iron alkyne derivatives and numerous X-ray studies have been reported [1,15]. The molecular structure of **5** is shown in Fig. 4 with selected bond lengths and angles. The Fe1–Fe2 distance of 2.552(2) Å is at the upper end of the range reported for the ferrole complexes [1]. It may be contrasted with an Fe–Fe distance of 2.515(1) Å in the parent ferrole $Fe_2(CO)_6(C_2H_2)_2$ [16] and is comparable to that observed in $Fe_2(CO)_6\{C_2(OH)(Et)\}_2$ [2.544(3) Å] [11].

The symmetrical ferracyclopentadiene ring results from the tail-to-tail coupling of the unsymmetrical terminal alkyne HC≡CPh. The C–C bond lengths within this ring are equivalent with values intermediate between single and double bonds [range 1.397(10)–1.416(11) Å]. This bond length equalisation has been explained by two different charge redistribution mecha-

nisms viz., π delocalisation and metal-induced σ, π rehybridisation [17].

As in the majority of structurally characterised ferrole complexes, **5** adopts the non-sawhorse conformation in which the CO and $P(OPh)_3$ ligands on the two iron atoms are staggered. The result is to place one of the CO ligands on Fe2 in a semi-bridging position where it is able to accept some of the electronic charge accumulated on the ring iron atom by the formal dative bond Fe2→Fe1. However, in **5** this interaction is highly asymmetric: the important dimensions are Fe2–C3 = 1.763(9), Fe1–C3 = 2.666(14) Å and Fe2–C3–O3 = 173.3(12)°. The Fe1–C3 distance has been observed to vary from 2.80 to 2.32 Å in different derivatives of this structural class [1]. Thus, the value of 2.67 Å in **5** is comparatively long. The Fe2–C3–O3 angle is larger than any previously reported suggesting that the structure of **5** may be intermediate between the sawhorse and non-sawhorse forms. Theoretical studies have shown that very small energy differences exist between the two geometries [18].

The solution-state spectroscopic data for **5** are in accordance with the solid state structure. The carbonyl region of the ^{13}C-NMR spectrum exhibits two doublet resonances (Table 2) which were assigned by comparison with literature data. The ferrole ring carbon resonances occur at δ 172.2 and 107.6: the more deshielded doublet signal was assigned to the ring carbons C5 and C8 directly bonded to Fe1 and strongly coupled to P1; the high-field singlet resonance was identified as the H-substituted carbon atoms C6 and C7 by a DEPT NMR experiment. These chemical shifts are in line with those observed in similarly substituted ferrole ring systems [19].

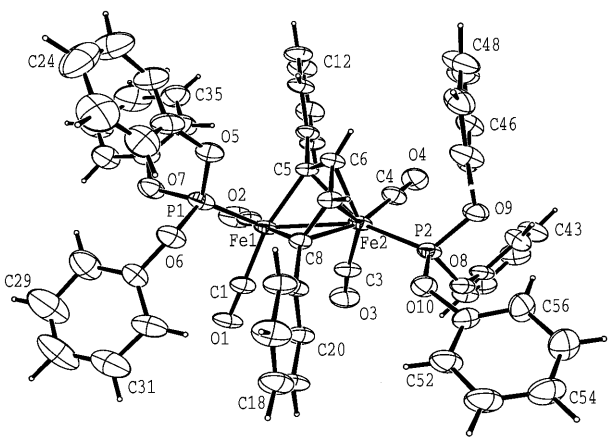

Fig. 4. ORTEX diagram of the molecular structure of **5**. Selected bond lengths (Å) and angles (°): Fe1–Fe2, 2.552(2); Fe1–P1, 2.105(4); Fe1–C1, 1.787(8); Fe1–C2, 1.773(8); Fe1–C3, 2.666(14); Fe1–C5, 1.988(7); Fe1–C8, 1.976(7); Fe2–P2, 2.148(3); Fe2–C3, 1.763(9); Fe2–C4, 1.757(10); Fe2–C5, 2.098(9); Fe2–C6, 2.099(9); Fe2–C7, 2.134(9); Fe2–C8, 2.159(9); C5–C6, 1.416(11); C6–C7, 1.397(10); C7–C8, 1.411(10); Fe1–C5–C6, 112.9(5); C5–C6–C7, 115.5(6); C6–C7–C8, 114.5(6); C7–C8–Fe1, 114.1(5); C8–Fe1–C5, 81.7(3); P1–Fe1–Fe2, 133.91(8); C1–Fe1–C2, 85.3(4); Fe1–Fe2–P2, 147.59(8); C3–Fe2–C4, 92.1(5).

The ferrole ring protons were not detected in the ^{1}H-NMR spectrum of **5**: possibly they are sufficiently deshielded to be obscured by the phenyl resonances of the $P(OPh)_3$ ligands.

Complex **5** was also accessible on treatment of $Fe(CO)_2\{P(OPh)_3\}_2$(PhCCPh) (**3a**) with HC≡CPh. The reaction was slow, occuring on a timescale comparable with that of the reaction of **2** with HC≡CPh, and affording the product, **5**, in similar yield. There was no spectroscopic evidence for the formation of ferrole species other than **5**: the coupling of PhC≡CPh and HC≡CPh was not observed.

There was also no evidence in the reactions of either **2** or **3a** with HC≡CPh for the formation of the vinylidene complex $Fe(CO)_2\{P(OPh)_3\}_2$(=C=CHPh) although Berke and co-workers have demonstrated the facility with which $Fe(CO)_2L_2$ $\{L = PEt_3, P(OMe)_3\}$ fragments induce this rearrangement [20].

3. Conclusions

The reaction of the orthometallated iron hydride **2** with alkynes has been shown to selectively afford either η^2-alkyne (**3**), maleoyl (**4**) or ferrole (**5**) derivatives depending on the alkyne chosen. The relatively high-yield syntheses of **4** are noteworthy since it is well documented that maleoyl formation from alkynes and metal carbonyls is severely limited by low selectivity [21]. In a future publication we will describe the reactivity of the complex **3a** and develop the mechanistic relationship between **3a**, **4** and **5**.

4. Experimental

4.1. General methods

All reactions were performed under N_2 using solvents predried by standard procedures. Alkynes and triphenylphosphite were purchased from Aldrich and used without further purification. Infrared spectra were recorded on a Perkin–Elmer 1710FT spectrometer. ^{1}H and ^{13}C{^{1}H}-NMR spectra were obtained on a Jeol JNM-GX270 FT-NMR spectrometer; ^{31}P{^{1}H}-NMR spectra were obtained on a Varian 300 MHz FT-NMR spectrometer. Elemental analyses were performed in the Microanalytical Laboratory, University College Dublin.

4.2. Synthesis of $Fe(CO)_3\{P(OPh)_3\}_2$ (1)

A solution of triphenylphosphite (40 ml, 152 mmol) and iron pentacarbonyl (10 ml, 76 mmol) in mesitylene (80 ml) was heated at reflux for 20 h. The reaction mixture was allowed to cool and was then filtered. Methanol (ca. 150 ml) was added to the filtrate and the

solution cooled in ice for ca. 1 h. The resulting precipitate was collected by filtration and washed with petroleum ether (40–60°C) to afford **1** as an analytically pure white solid (37.5 g, 65% yield). M.p. 121–122°C. IR (cm^{-1}) ν_{CO} 1927(10), 1917(9.6) (KBr). $^{31}P\{^{1}H\}$-NMR 182.0 (s).

4.3. Synthesis of $HFe(CO)_2\{P(OPh)_3\}\{(PhO)_2POC_6H_4\}$ (2)

A stirred solution of **1** (0.500 g, 0.66 mmol) in toluene (50 ml) was cooled in an ice–water bath and irradiated with a 125 W mercury vapour lamp until the starting material was consumed (typically 1–2 h) as determined by IR spectroscopy. The resulting solution of **2** was used directly in further reactions. IR (cm^{-1}) ν_{CO} 2034(10), 1984(7.8) (toluene). ^{1}H-NMR (d_6-benzene) 7.8–6.0 (m, Ph), −9.36 (br m, Fe–H).

4.4. General procedure for the synthesis of 3–5

A stoichiometric amount of the required alkyne was added to a solution of **2** prepared as described above. Approximately 0.01 g of the appropriate Lewis acid ($ZnCl_2 \cdot nH_2O$ or anhydrous $MgSO_4$) was introduced and the resulting mixture was allowed to stir at r.t. overnight. The mixture was filtered, concentrated to dryness and the residue was purified by column chromatography on alumina. Elution with 1:1 hexanes–dichloromethane afforded a pale red material containing unidentified by-products of the photolysis. The required product was obtained as a yellow–orange material on elution with dichloromethane or THF. Recrystallisation from toluene–hexane or CH_2Cl_2–hexane mixtures afforded the product as a yellow solid.

4.5. Reaction of 3a and HC≡CPh

Phenylacetylene (0.03 ml, 0.27 mmol) was added to a solution of **3a** (0.20 g, 0.220 mmol) in toluene (15 ml) and the mixture was allowed to stir overnight at r.t. It was concentrated and the residue was chromatographed on alumina as described above to give **5** (38% yield).

4.6. X-ray data collection and structure refinement

X-ray quality single crystals of **3a**, **4c** and **5** were grown from either benzene–hexane or toluene–hexane solutions. X-ray data were collected on an Enraf Nonius CAD4 diffractometer with graphite monochromatised Mo–K_α radiation ($\lambda = 0.7093$ Å) at 293(2) K. Data were corrected for Lorentz and polarisation ef-

Table 3
Summary of crystal data and details of the data collection and refinement for **3a**, **4c** and **5**

Complex	3a	4c	5
Empirical formula	$C_{52}H_{40}FeO_8P_2$	$C_{48}H_{44}FeO_{12}P_2$	$C_{56}H_{42}Fe_2O_{10}P_2$
Molecular weight (g mol^{-1})	910.63	930.62	1048.59
Colour, habit	Orange, block	Yellow, block	Yellow, block
Crystal size (mm)	$0.50 \times 0.38 \times 0.35$	$0.43 \times 0.32 \times 0.24$	$0.42 \times 0.37 \times 0.25$
Crystal system	Monoclinic	Triclinic	Monoclinic
Space group	$C2/c$	$P\bar{1}$	$P2_1/c$
a (Å)	25.022(2)	9.214(2)	11.133(2)
b (Å)	10.005(2)	12.398(2)	47.549(10)
c (Å)	19.228(2)	20.413(3)	11.451(2)
α (°)	90	90.720(10)	90
β (°)	111.88(2)	97.00(1)	118.39(10)
γ (°)	90	99.97(2)	90
Volume (Å^3)	4466.9(11)	2278.2(7)	5332.7(17)
Z	4	2	4
D_{calc} (Mg m^{-3})	1.354	1.357	1.403
$F(000)$	1888	968	2328
μ (mm^{-1})	0.465	0.463	0.665
θ range for data collection	2–25	2–25	2–25
hkl range	−3–32, −3–13, −15–23	0–5, –18–18, −30–30	0–5, −14–34, −16–14
Reflections collected	4944	8867	7480
Unique reflections	4542	7762	6896
Reflections with $[I>2\sigma(I)]$	3769	3543	5738
Data/restraints/parameters	4542/0/285	7762/214/725	6896/144/758
Goodness-of-fit	1.078	0.891	1.362
Final R indices $[I>2\sigma(I)]$	$R_1 = 0.045$, $wR_2 = 0.129$	$R_1 = 0.060$, $wR_2 = 0.147$	$R_1 = 0.108$, $wR_2 = 0.297$
R indices (all data)	$R_1 = 0.051$, $wR_2 = 0.134$	$R_1 = 0.140$, $wR_2 = 0.174$	$R_1 = 0.123$, $wR_2 = 0.309$
Density range in final Δ-map (e Å^{-3})	1.01, −0.33	0.58, −0.58	1.72, −1.32

fects but not for absorption. The structures were solved by direct methods, SHELXS-86 [22], and refined by full-matrix least squares using SHELXL-97 [23]. Hydrogen atoms were included in calculated positions using the default SHELXL-97 C–H settings with displacement parameters 20–50% larger than the atoms to which they were attached (depending on carbon type). Calculations were performed on a Silicon Graphics R4000 computer. Details of the X-ray data collection and structure refinement are summarised in Table 3.

In the penultimate stages of refinement of **4c** {when $R[F^2 > 2\sigma(F^2)]$ was 0.08}, it was noted that considerable disorder is present in the maleoyl residue. The $CH(OCH_2CH_3)_2$ group (attached to the alkenyl C4) has large displacement parameters; this is not uncommon for structures incorporating the acetal group [24]. At this refinement stage, the highest peaks in the residual electron density map (ca. 1 e $Å^{-3}$) lay in close proximity to the methyl group C12 (bonded to the neighbouring alkenyl C5) at distances ca. 1.3–1.6 Å and angles of 100–120° (in a chain) suggesting that either residual solvent or some component of disorder was present in this volume element of the crystal structure. These residual peaks were initially included as minor ethoxy sites in subsequent refinement cycles with a fixed site occupancy factor of 0.25. A model of the minor acetal site at the major methyl position (s.o.f. = 0.75) was fashioned using DFIX bond/angle restraints in combination with moderate DELU/ISOR SHELXL-97 controls anchored at the alkenyl C4=C5 part of the ligand. In the succeeding refinement cycles, the site occupancy factors of the major and minor acetal site refined freely to 0.805 and 0.195, respectively, and were fixed in the final least-squares refinement cycles. Disorder in one of the ethoxy groups in the major maleoyl site was noted (0.630/0.175) and modelled; disorder in one of the phenyl rings was also present in {C43A,…C48A/C43B,…C48B} which refined to 63 and 37% occupancy factors, respectively. The *R*-factor drops from 6.9 to 6.0% by the successful modelling of the acetal/phenyl ring disorder giving a final shift/error ratio of 0.02.

The crystal of **5** decayed by 60% during the data collection as noted from the intensities of the three standard reflections thus limiting the precision of our results; however, the overall structure of **5** was unequivocally established. In the crystal structure, solvent of crystallisation was obvious at an intermediate stage of the refinement process; this was successfully modelled as three orientations of a benzene solvent of crystallisation, which is loosely held in a large void in the crystal lattice.

5. Supplementary material

Crystallographic data for the structural analyses have been deposited with the Cambridge Crystallographic Data Centre, CCDC no. 143982, 143983 and 143984 for compounds **3a**, **4c** and **5**, respectively. Copies of this information may be obtained free of charge from The Director, CCDC, 12 Union Road, Cambridge, CB2 1EZ, UK (Fax: +44-1223-336033; e-mail: deposit@ccdc.cam.ac.uk or www: http://www.ccdc.cam.ac.uk).

References

[1] W.R. Fehlhammer, H. Stolzenberg, in: G. Wilkinson, F.G.A. Stone, E.W. Abel (Eds.), Comprehensive Organometallic Chemistry, vol. 4, Pergamon, Oxford, 1983, p. 545.
[2] W. Hubel, in: I. Wender, P. Pino (Eds.), Organic Syntheses via Metal Carbonyls, vol. I, Wiley, New York, 1968, p. 273.
[3] (a) R.L. Keiter, E.A. Keiter, C.A. Boecker, D.R. Miller, K.H. Hecker, Inorg. Synth. 31 (1997) 210. (b) J.J. Brunet, F.B. Kindela, D. Neibecker, Inorg. Synth. 29 (1992) 151.
[4] H.L. Conder, M.Y. Darensbourg, J. Organomet. Chem. 67 (1974) 93.
[5] M. Barrow, N.L. Cromhout, D. Cunningham, A.R. Manning, P. McArdle, J. Renze, J. Organomet. Chem. 563 (1998) 201.
[6] S.M. Grant, A.R. Manning, J. Chem. Soc. Dalton Trans. (1979) 1789.
[7] M. Knorr, U. Schubert, J. Organomet. Chem. 365 (1989) 151.
[8] F. Meier-Brocks, R. Albrecht, E. Weiss, J. Organomet. Chem. 439 (1992) 65.
[9] P. McArdle, J. Appl. Crystallogr. 28 (1995) 65.
[10] F.W.B. Einstein, K.G. Tyers, D. Sutton, Organometallics 4 (1985) 489 and references therein.
[11] S. Aime, L. Milone, E. Sappa, A. Tiripicchio, A.M. Manotti Lanfredi, J. Chem. Soc. Dalton Trans. (1979) 1664.
[12] R.C. Pettersen, R.A. Levenson, Acta Crystallogr. Sect. B 32 (1976) 723.
[13] A.G. Orpen, L. Brammer, F.H. Allen, O. Kennard, D.G. Watson, R.Taylor, in: H.B. Burgi, J.D. Dunitz (Eds.), Structure Correlation, Vol. 2, VCH, Weinheim, Germany, 1994, Appendix A.
[14] (a) M.H. Cheng, G.H. Lee, S.M. Peng, R.S. Liu, Organometallics 10 (1991) 3600. (b) M.H. Cheng, H.G. Shu, G.H. Lee, S.M. Peng, R.S. Liu, Organometallics 12 (1993) 108.
[15] For recent structural determinations: (a) R. Calderon, H. Vahrenkamp, J. Organomet. Chem. 555 (1998) 113. (b) D. Seyferth, C.M. Archer, J.C. Dewan, Organometallics 10 (1991) 3759.
[16] G. Detlaff, E. Weiss, J. Organomet. Chem. 108 (1976) 213.
[17] (a) M. Casarin, D. Ajo, A. Vittadini, D.E. Ellis, G. Granozzi, R. Bertoncello, D. Osella, Inorg. Chem. 26 (1987) 2041. (b) A. Marzotto, M. Biagini, A. Ciccarese, A. Clemente, Acta Crystallogr. Sect. C 47 (1991) 96.
[18] D.L. Thorn, R. Hoffmann, Inorg. Chem. 17 (1978) 126.
[19] L.J. Todd, J.P. Hickey, J.R. Wilkinson, J.C. Huffman, K. Folting, J. Organomet. Chem. 112 (1976) 167 and references therein.
[20] C. Gauss, D. Veghini, H. Berke, Chem. Ber. 130 (1997) 183.
[21] (a) L.S. Liebeskind, C.F. Jewell, J. Organomet. Chem. 285 (1985) 305. (b) R. Victor, V. Vsieli, S. Sarel, J. Organomet. Chem. 129 (1977) 387. (c) R.C. Petterson, J.L. Cihonski, F.R. Young, R.A. Levenson, J. Chem. Soc. Chem. Commun. (1975) 370.
[22] G.M. Sheldrick, Acta Crystallogr. Sect. A 46 (1990) 467.
[23] G.M. Sheldrick, SHELXL-97, A Program for the Refinement of Crystal Structures, University of Göttingen, Germany, 1997.
[24] P. Butler, J.F. Gallagher, A.R. Manning, Inorg. Chem. Commun. 1 (1998) 343.